Applied Mathematics of Interconnected Phenomena

https://engineering-journals.org/journals/amip/

Parametric Entrainment and Amplitude Enhancement in a Van der Pol Oscillator with State-Multiplicative Periodic Forcing: A Rigorous Averaging Analysis

Adrián Valverde Mateo[†]

Departamento de Ingeniería y Tecnología de Computadores
Facultad de Informática, Campus de Espinardo
Universidad de Murcia, Spain

Submission Info

Communicated by Z. Sabir
Received 15 September 2026
Accepted 21 October 2026
Available online 30 October 2026

Abstract

We study the Van der Pol oscillator $\ddot{x}-\mu(1-x^2)\dot{x}+x=Fx\cos\omega t$, in which the external excitation is multiplied by the state, so that the forcing acts parametrically and vanishes at the origin. Written as a Van der Pol–Mathieu oscillator, the equation admits a complete analysis of its principal 2:1 resonance, and every result below is proved. First, the trivial solution is unstable for every F and ω when $\mu>0$, with Floquet exponents $\mu/2\pm s$, where s is the exponent of an associated Mathieu equation; the sum of the exponents of any periodic orbit equals $\mu(1-\langle x^2\rangle)$, and every periodic orbit satisfies an exact power balance. Second, the first-order averaged flow is triangular, and the substitution $u=a^{-2}$ makes its amplitude equation linear; this yields *global* statements. Inside the tongue $|\omega-2|<F/2$ all solutions except one are attracted to a subharmonic orbit of amplitude $a_+=2\sqrt{1+\mathscr{D}/(2\mu)}>2$, $\mathscr{D}=\sqrt{F^2-4(\omega-2)^2}$, while a saddle orbit of amplitude $a_-=2\sqrt{1-\mathscr{D}/(2\mu)}$ exists if and only if $\mathscr{D}<2\mu$; both merge with the origin on the hyperbola $F^2=4(\omega-2)^2+4\mu^2$. Outside the tongue a unique attracting orbit of the slow flow, with closed-form amplitude envelope, transverse rate μ and phase-rotation frequency $\kappa/2$, is obtained. Third, by averaging and normal hyperbolicity these objects persist in the full equation as a hyperbolic subharmonic periodic orbit, a saddle periodic orbit and an attracting invariant torus, respectively. Dimensional design rules follow. An appendix, clearly separated from the proofs, confirms the first-order predictions and, for strong forcing, indicates chaos; two precise open problems are formulated.

Keywords: Van der Pol oscillator; Van der Pol–Mathieu equation; parametric resonance; averaging method; Arnold tongue; Floquet theory; invariant torus; subharmonic orbits.
AMS 2010 codes: 34C15, 34C29, 34C25, 34D20, 37G15.

1 Introduction

The Van der Pol oscillator [1] is the prototype of a self-sustained oscillator: a nonlinear damping term that is negative for small and positive for large displacements creates a unique, globally attracting limit cycle. Its

[†]Corresponding author.
Email address: a.valverde@um.es

© 2026 Adrián Valverde Mateo, published by Applied Mathematics of Interconnected Phenomena.

This work is licensed under the Creative Commons Attribution alone 4.0 License.

ISSN pending
10.66833/AMIP-2026-0002

response to an external periodic force is classical and leads to entrainment (frequency locking), quasi-periodic motion and chaos [5, 6]. In the standard setting the force is additive, $F\cos\omega t$. In many physical systems, however, the excitation modulates a system parameter and is therefore multiplied by the state. The simplest such model is

$$\ddot{x}-\mu(1-x^2)\dot{x}+x=F\,x\cos\omega t, \qquad \mu>0,\ F\geq 0,\ \omega>0. \tag{1}$$

Here the forcing vanishes when the oscillator crosses the origin and grows with the displacement. Equation (1) is the *Van der Pol–Mathieu* equation: moving the right-hand side to the left gives $\ddot{x}-\mu(1-x^2)\dot{x}+(1-F\cos\omega t)x=0$, i.e. a Mathieu oscillator [2–4] with Van der Pol damping. Quasi-periodic phenomena, 2:1 and 1:1 frequency locking, and related resonances of this equation have been investigated in several regimes [7–10]. More recent work has addressed oscillators with combined self-, parametric and external excitation [11, 12], including the quasi-periodic spectra of the externally forced Van der Pol–Mathieu equation [12], as well as the resonances of the forced Van der Pol equation with parametric damping [13] and parametric amplification in the Mathieu equation [14]. Applications include dust-acoustic oscillations in dusty plasmas [15]; see Section 4. Our goal is a *complete, rigorous* description of the principal parametric resonance $\omega\approx 2$, in which every statement is proved.

Contributions.

(i) *Exact theory* (Section 2). The trivial solution is unstable for all (F,ω) when $\mu>0$, with Floquet exponents $\mu/2\pm s$ (s the exponent of a Mathieu equation); it is a saddle iff $s>\mu/2$. Every periodic orbit satisfies an exact power balance and $\lambda_1+\lambda_2=\mu(1-\langle x^2\rangle)$.

(ii) *Global slow flow* (Section 3). The averaged system is triangular, and $u=a^{-2}$ linearises its amplitude equation. This gives global (not merely local) statements: basins, explicit amplitudes, explicit exponents, an explicit amplitude envelope outside the tongue, and the structure of the locking transition.

(iii) *Persistence* (Section 3.4). By averaging and normal hyperbolicity, the slow-flow objects persist in (1) for small forcing and damping.

(iv) *Design rules* (Section 4). Dimensional consequences for amplification and entrainment, with the exact rescaling to physical variables.

(v) *Numerical appendix* (Appendix 5). Numerical evidence, kept separate from the proofs, that tests the first-order theory, explores strong forcing, and leads to two open problems.

2 Exact properties of the equation

Let $T=2\pi/\omega$. System (1) is the planar, T-periodic system $\dot{x}=v$, $\dot{v}=\mu(1-x^2)v-x+Fx\cos\omega t$.

Proposition 1 (Symmetries)**.** *(i) (1) is invariant under $x\mapsto -x$. (ii) It is invariant under $t\mapsto t+T$. (iii) If $x(t)$ is a solution satisfying $x(t+T)=-x(t)$, then x has minimal period $2T=4\pi/\omega$ and is a fixed point of the map $R\circ\Pi_T$, where Π_T is the stroboscopic map and $R(x,v)=(-x,-v)$.*

Proof. (i) and (ii) are immediate since x enters only through odd terms and $F\cos\omega t$ is T-periodic. (iii) follows from $x(t+2T)=-x(t+T)=x(t)$ and the definition of Π_T. □

Proposition 2 (The trivial solution)**.** *For every $F\geq 0$ and $\omega>0$, $x\equiv 0$ is a solution. Let $\rho_{1,2}$ be the Floquet multipliers over one period T of the Mathieu equation*

$$y''+\Big(1-\tfrac{\mu^2}{4}-F\cos\omega t\Big)y=0, \qquad \rho_1\rho_2=1. \tag{2}$$

Then the Floquet multipliers of the linearisation of (1) at $x=0$ are $e^{\mu T/2}\rho_{1,2}$, and the Floquet exponents are $\lambda_\pm=\mu/2\pm s$, where $e^{sT}=\max|\rho_j|$, $s\geq 0$. Consequently, for $\mu>0$:

(a) $\lambda_+ + \lambda_- = \mu$ *and* $\lambda_+ \geq \mu/2 > 0$*: the origin is unstable for all* F, ω*;*

(b) the origin is a saddle if and only if $s > \mu/2$*, and an unstable node or focus if and only if* $s < \mu/2$ *(with the borderline case* $s = \mu/2$ *degenerate).*

Proof. The linearisation is $\ddot{x} - \mu\dot{x} + (1 - F\cos\omega t)x = 0$. The substitution $x = e^{\mu t/2}y$ removes the first-derivative term and gives (2). Since (2) has no first-derivative term, the Liouville formula gives $\rho_1\rho_2 = 1$. The multipliers of the x-equation are therefore $e^{\mu T/2}\rho_j$, whose moduli are $e^{(\mu/2 \pm s)T}$. This yields the exponents and (a). For (b), $\lambda_- = \mu/2 - s < 0$ iff $s > \mu/2$. □

Proposition 3 (Liouville identity)**.** *Let* $x_*(t)$ *be a periodic solution of period* P *with Floquet exponents* λ_1, λ_2*. Then*

$$\lambda_1 + \lambda_2 = \frac{1}{P}\int_0^P \mu\left(1 - x_*(t)^2\right) \mathrm{d}t. \tag{3}$$

Proof. The trace of the Jacobian of the vector field is $\mu(1 - x^2)$; apply Liouville's formula to the monodromy matrix, $\det M = \exp\int_0^P \mu(1 - x_*^2)\,\mathrm{d}t$. □

In particular, $\lambda_1 + \lambda_2 = \mu\left(1 - \langle x_*^2\rangle\right)$, so a periodic orbit contracts area on average iff its mean square exceeds 1.

Proposition 4 (Exact power balance)**.** *Let* x_* *be a periodic solution of period* P *(a multiple of* T*). With* $E = \frac{1}{2}(\dot{x}^2 + x^2)$*,*

$$\mu\langle(1 - x_*^2)\dot{x}_*^2\rangle + F\langle x_*\dot{x}_*\cos\omega t\rangle = 0. \tag{4}$$

Proof. $\dot{E} = \dot{x}(\ddot{x} + x) = \mu(1 - x^2)\dot{x}^2 + Fx\dot{x}\cos\omega t$, and $\int_0^P \dot{E}\,\mathrm{d}t = 0$ by periodicity. □

The balance states that the power injected by the self-excitation $\mu(1 - x^2)\dot{x}^2$ is exactly compensated by the work of the parametric term. At first order it reproduces the equilibrium condition $\mu(1 - a^2/4) = (F/2)\sin 2\varphi$ of the averaged system (Theorem 6).

3 Averaging analysis of the principal resonance

3.1 The averaged system

Introduce the scaling $\mu = \varepsilon\mu_0$, $F = \varepsilon f$, $\omega = 2 + \varepsilon\sigma$ with $0 < \varepsilon \ll 1$, and set $\nu = \omega/2$. Equation (1) reads $\ddot{x} + \nu^2 x = G$ with $G = \mu(1 - x^2)\dot{x} + (\nu^2 - 1)x + Fx\cos 2\nu t$, and $\nu^2 - 1 = (\omega - 2) + O(\varepsilon^2)$. The substitution $x = a\cos\psi$, $\dot{x} = -a\nu\sin\psi$, $\psi = \nu t + \varphi$ is exact for $a > 0$ and gives

$$\dot{a} = -\frac{G}{\nu}\sin\psi, \qquad a\dot{\varphi} = -\frac{G}{\nu}\cos\psi,$$

with $G = O(\varepsilon)$, i.e. the standard form for first-order averaging [16, 17]. Using $2\nu t = 2\psi - 2\varphi$ and $\nu = 1 + O(\varepsilon)$,

$$G = -\mu a\sin\psi\,(1 - a^2\cos^2\psi) + (\omega - 2)\,a\cos\psi + Fa\cos\psi\cos(2\psi - 2\varphi) + O(\varepsilon^2).$$

The needed averages over ψ are $\langle\sin^2\psi\rangle = \frac{1}{2}$, $\langle\sin^2\psi\cos^2\psi\rangle = \frac{1}{8}$, $\langle\sin\psi\cos\psi\rangle = 0$, $\langle\sin\psi\cos\psi(1 - a^2\cos^2\psi)\rangle = 0$, $\langle\sin\psi\cos\psi\cos(2\psi - 2\varphi)\rangle = \frac{1}{4}\sin 2\varphi$, $\langle\cos^2\psi\cos(2\psi - 2\varphi)\rangle = \frac{1}{4}\cos 2\varphi$, $\langle\cos^2\psi\rangle = \frac{1}{2}$. Hence $-\langle G\sin\psi\rangle = \frac{1}{2}\mu a(1 - a^2/4) - \frac{1}{4}Fa\sin 2\varphi$ and $-\langle G\cos\psi\rangle = -\frac{1}{2}(\omega - 2)a - \frac{1}{4}Fa\cos 2\varphi$, and the *averaged system* is

$$\dot{a} = \frac{a}{2}\left[\mu\left(1 - \frac{a^2}{4}\right) - \frac{F}{2}\sin 2\varphi\right], \qquad \dot{\varphi} = -\frac{1}{2}\left[(\omega - 2) + \frac{F}{2}\cos 2\varphi\right]. \tag{5}$$

By the first-order averaging theorem [16, Ch. 2], solutions of (1) and (5) with the same initial data and $a \geq a_0 > 0$ differ by $O(\varepsilon)$ on time intervals of length $O(1/\varepsilon)$. We use the quantities

$$\mathscr{D} = \sqrt{F^2 - 4(\omega - 2)^2}\ \ (|\omega - 2| \leq F/2), \qquad \kappa = \sqrt{(\omega - 2)^2 - F^2/4}\ \ (|\omega - 2| \geq F/2).$$

Lemma 5 (Triangular structure and linearisation)**.** *The φ-equation in (5) does not involve a. With $u = a^{-2}$, system (5) is equivalent, for $a > 0$, to*

$$\dot{\varphi} = -\tfrac{1}{2}\, q(\varphi), \qquad \dot{u} = -g(\varphi)\, u + \frac{\mu}{4}, \tag{6}$$

where $q(\varphi) = (\omega - 2) + \frac{F}{2}\cos 2\varphi$ and $g(\varphi) = \mu - \frac{F}{2}\sin 2\varphi$. For fixed $\varphi(t)$ the u-equation is linear.

Proof. $\dot{u} = -2\dot{a}/a^3 = -u\big[\mu - \mu a^2/4 - (F/2)\sin 2\varphi\big] = -gu + \mu/4$. □

Note that the substitution maps the cubic nonlinearity of the Van der Pol damping into an inhomogeneous constant, so all global questions reduce to the scalar circle flow $\dot{\varphi} = -q/2$ followed by a linear equation. Moreover, if $(a(t), \varphi(t))$ solves (5) for the detuning $\omega - 2$, then $(a(t), \frac{\pi}{2} - \varphi(t))$ solves (5) for the detuning $-(\omega - 2)$ (direct substitution, using $\sin(\pi - 2\varphi) = \sin 2\varphi$ and $\cos(\pi - 2\varphi) = -\cos 2\varphi$), so one may restrict attention to $\omega \geq 2$ whenever convenient.

3.2 Global dynamics of the averaged system

Theorem 6 (Locked regime)**.** *Let $|\omega - 2| < F/2$ (so $\mathscr{D} > 0$) and $\mu > 0$. The circle flow $\dot{\varphi} = -q/2$ has exactly two equilibria modulo π: φ_s with $\sin 2\varphi_s = -\mathscr{D}/F$, which is stable, and φ_u with $\sin 2\varphi_u = +\mathscr{D}/F$, which is unstable; both satisfy $\cos 2\varphi = -2(\omega - 2)/F$. System (5) has the following equilibria with $a \geq 0$.*

(a) The origin $a = 0$.

(b) The node *$N = (a_+, \varphi_s)$ with*

$$a_+ = 2\sqrt{1 + \frac{\mathscr{D}}{2\mu}} > 2, \tag{7}$$

with eigenvalues $\lambda_1^N = -(\mu + \mathscr{D}/2)$ and $\lambda_2^N = -\mathscr{D}/2$ (the equilibrium is a stable node).

(c) If and only if $\mathscr{D} < 2\mu$, the saddle *$S = (a_-, \varphi_u)$ with*

$$a_- = 2\sqrt{1 - \frac{\mathscr{D}}{2\mu}} \in (0, 2), \tag{8}$$

with eigenvalues $\lambda_1^S = -(\mu - \mathscr{D}/2)$ and $\lambda_2^S = +\mathscr{D}/2$.

Every solution with $a(0) > 0$ and $\varphi(0) \not\equiv \varphi_u \pmod{\pi}$ converges to N. On the line $\varphi \equiv \varphi_u$, solutions converge to S if $\mathscr{D} < 2\mu$, tend to the origin if $\mathscr{D} \geq 2\mu$ (with $a(t) \sim t^{-1/2}$ when $\mathscr{D} = 2\mu$). The sum of the eigenvalues is $-(\mu + \mathscr{D})$ at N and $-(\mu - \mathscr{D})$ at S.

Proof. The equilibria of the circle flow satisfy $q = 0$, i.e. $\cos 2\varphi = -2(\omega - 2)/F$; they exist iff $|\omega - 2| \leq F/2$ and then $\sin 2\varphi = \pm\mathscr{D}/F$. The derivative of $-q/2$ is $(F/2)\sin 2\varphi$, negative at φ_s and positive at φ_u. At an equilibrium φ_* the u-equation is $\dot{u} = -g_* u + \mu/4$ with $g_* = \mu - (F/2)\sin 2\varphi_*$. At φ_s: $g_s = \mu + \mathscr{D}/2 > 0$ and $u \to \mu/(4g_s) = 1/[4(1 + \mathscr{D}/2\mu)]$, i.e. (7). At φ_u: $g_u = \mu - \mathscr{D}/2$; if $g_u > 0$ then $u \to \mu/(4g_u)$, i.e. (8); if $g_u < 0$ then $u \to \infty$ exponentially (so $a \to 0$); if $g_u = 0$ then $\dot{u} = \mu/4$, $u = \mu t/4 + u_0$ and $a \sim t^{-1/2}$. For all initial data with $\varphi(0) \neq \varphi_u$ the circle flow converges to φ_s, and the linear u-equation then converges to $\mu/(4g_s)$ by variation of constants, since $g(\varphi(t)) \to g_s > 0$. The Jacobian at an equilibrium with $a_* > 0$ in the variables (a, φ) is triangular: $\partial_a \dot{a} = -\mu a_*^2/4$, $\partial_\varphi \dot{\varphi} = (F/2)\sin 2\varphi_*$, $\partial_a \dot{\varphi} = 0$. At N: $-\mu a_+^2/4 = -(\mu + \mathscr{D}/2)$ and $(F/2)\sin 2\varphi_s = -\mathscr{D}/2$. At S: $-\mu a_-^2/4 = -(\mu - \mathscr{D}/2)$ and $+\mathscr{D}/2$. □

Remark 1. The locked amplitude exceeds that of the unforced limit cycle: $a_+ > 2$ in the whole tongue, with maximum $a_+^{\max} = 2\sqrt{1 + F/(2\mu)}$ at $\omega = 2$, and $a_+ \to 2$ at the edges. In particular the forcing *increases* the amplitude of the oscillation rather than destroying the cycle. The saddle amplitude satisfies $a_- < 2 < a_+$.

Theorem 7 (Quasi-periodic regime)**.** *Let* $|\omega-2|>F/2$*. Then* φ *rotates monotonically with mean angular frequency* $\kappa/2$*: precisely,* φ *advances by* π *in the time* $T_\varphi=2\pi/\kappa$*. System* (5) *has a unique periodic orbit* Γ *with* $a>0$*, given by* $u=u_\Gamma(\varphi)$ *which, for* $\omega>2$*, is*

$$u_\Gamma(\varphi)=\frac{\mu}{2}\,\frac{q(\varphi)\,e^{2\mu\Theta(\varphi)}}{1-e^{-2\pi\mu/\kappa}}\int_\varphi^{\varphi+\pi}\frac{e^{-2\mu\Theta(s)}}{q(s)^2}\,\mathrm{d}s,\qquad \Theta(\varphi)=\int_0^\varphi\frac{\mathrm{d}s}{q(s)},\tag{9}$$

and $a_\Gamma(\varphi)=u_\Gamma^{-1/2}$ *(the case* $\omega<2$ *follows from the symmetry noted above). Every solution with* $a(0)>0$ *converges to* Γ *with*

$$|u(t)-u_\Gamma(\varphi(t))|\le Ce^{-\mu t}\quad\text{(for suitable } C\text{)},$$

and the time average of $g(\varphi(t))$ *along* Γ *equals exactly* μ*.*

Proof. Since $|\omega-2|>F/2$, q has a fixed sign, so φ is monotone. With $\theta=2\varphi$, $\int_0^\pi \mathrm{d}\varphi/q=\frac{1}{2}\int_0^{2\pi}\mathrm{d}\theta/((\omega-2)+(F/2)\cos\theta)=\pi/\kappa$ for $\omega>2$, so φ advances by π in time $T_\varphi=2\int_0^\pi\mathrm{d}\varphi/|q|=2\pi/\kappa$. Use φ as the independent variable: $\mathrm{d}u/\mathrm{d}\varphi=(2/q)(gu-\mu/4)$. Because $\mathrm{d}(\ln q)/\mathrm{d}\varphi=-F\sin2\varphi/q$, we have $\int 2g/q\,\mathrm{d}\varphi=2\mu\Theta+\ln q$, so $I=qe^{2\mu\Theta}$ is an integrating factor and $(u/I)'=-\mu/(2qI)=-\mu\,e^{-2\mu\Theta}/(2q^2)$. Since $\Theta(\varphi+\pi)=\Theta(\varphi)+\pi/\kappa$, the unique π-periodic positive solution is (9). For another solution, $w=u-u_\Gamma(\varphi(t))$ obeys $\dot w=-g(\varphi(t))\,w$. Over one rotation (φ changes by π in absolute value, in time T_φ) we have $\int g\,\mathrm{d}t=\int(2g/q)\,\mathrm{d}\varphi=2\mu\int\mathrm{d}\varphi/q+[\ln q]=2\mu\pi/\kappa=\mu T_\varphi$, because $\ln q$ is periodic. Thus the Floquet multiplier of the linear equation for w over one rotation is $e^{-\mu T_\varphi}$, which gives $w=O(e^{-\mu t})$ and shows that the time average of g equals μ. □

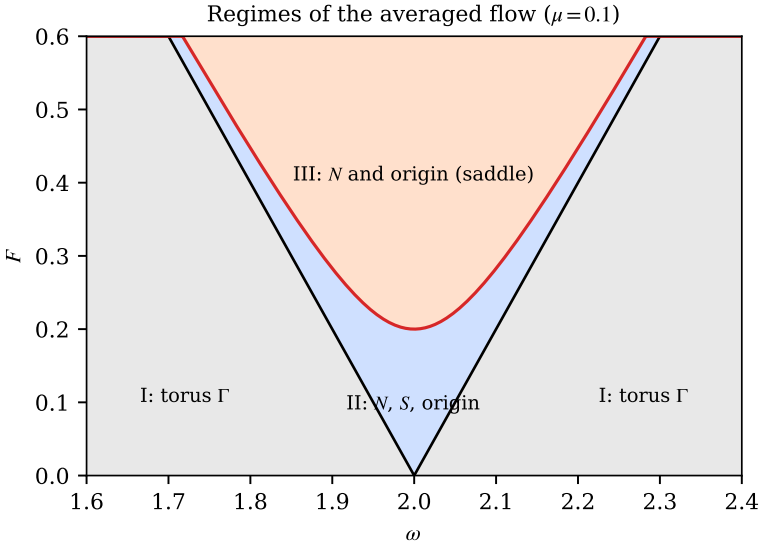

Fig. 1 Regimes of the averaged flow in the (ω,F)-plane for $\mu=0.1$ (drawn from the closed formulas): I, $|\omega-2|>F/2$ (Theorem 7); II, $|\omega-2|<F/2$ and $\mathscr{D}<2\mu$ (origin, saddle S, node N); III, $\mathscr{D}>2\mu$ (origin a saddle, node N). Black: $F=2|\omega-2|$; red: $F=2\sqrt{(\omega-2)^2+\mu^2}$.

Remark 2 (Structure of the locking transition). Inside the tongue the unstable manifold of S consists of two arcs, each a graph over the φ-circle (since φ is monotone along them) and each converging to N by Theorem 6; together with S and N they form an invariant closed curve. As $|\omega-2|\uparrow F/2$ one has $\mathscr{D}\downarrow 0$ and N, S coalesce at $a=2$, because $a_\pm\to 2$; for $|\omega-2|>F/2$ no equilibrium exists and the slow phase rotates with frequency $\kappa/2\to 0$ as the boundary is approached, i.e. like the square root of the distance to it, since $\kappa^2=(|\omega-2|-F/2)(|\omega-2|+F/2)$. This is the structure of a saddle–node bifurcation on an invariant circle.

Remark 3 (Hyperbola). Inside the tongue the saddle exists iff $\mathscr{D} < 2\mu$, i.e. iff $F^2 < 4(\omega-2)^2 + 4\mu^2$; on the curve $F = 2\sqrt{(\omega-2)^2+\mu^2}$ one has $a_- \to 0$ and S merges with the origin. By Lemma 8 below, this is exactly where the smaller eigenvalue $\mu/2 - \mathscr{D}/4$ of the origin vanishes, and beyond it the origin is a saddle of the averaged flow.

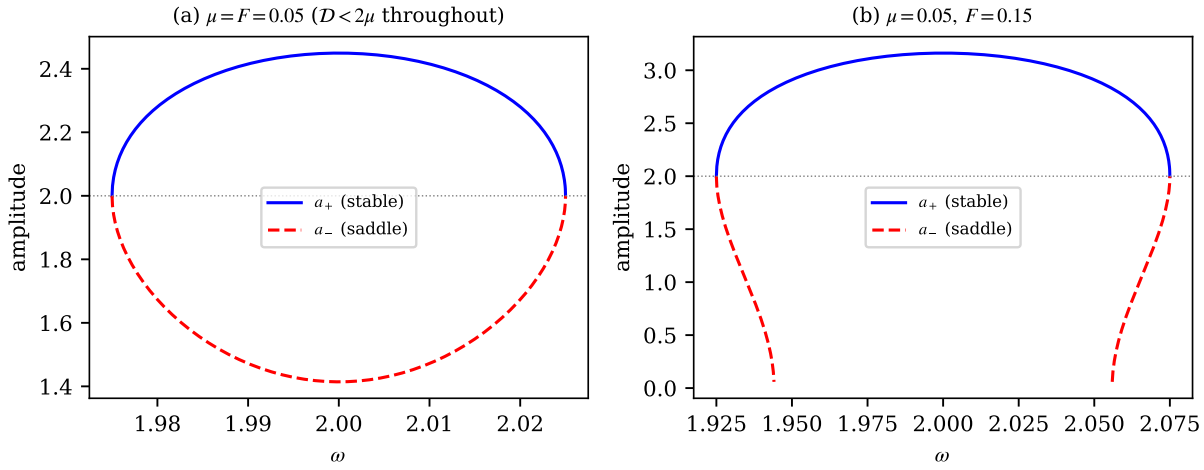

Fig. 2 Amplitudes a_+ (blue) and a_- (red dashed) of Theorem 6 versus ω (closed formulas). (a) $\mathscr{D} < 2\mu$ throughout, so the saddle branch closes the loop at $a = 2$. (b) The saddle branch reaches the origin where $\mathscr{D} = 2\mu$.

3.3 The origin in the averaged flow

Lemma 8 (Origin). *In the variables $\xi = a\cos\varphi$, $\eta = a\sin\varphi$ the linearisation of (5) at the origin is*

$$\begin{pmatrix}\dot\xi\\ \dot\eta\end{pmatrix} = \frac{1}{2}\begin{pmatrix}\mu & (\omega-2)-F/2\\ -(\omega-2)-F/2 & \mu\end{pmatrix}\begin{pmatrix}\xi\\ \eta\end{pmatrix},$$

with eigenvalues $\mu/2 \pm \mathscr{D}/4$ if $|\omega-2| \le F/2$ and $\mu/2 \pm i\kappa/2$ if $|\omega-2| \ge F/2$. Hence the origin is a saddle iff $\mathscr{D} > 2\mu$. For the full equation, the Floquet exponents of the origin are ε times these eigenvalues, up to $O(\varepsilon^2)$.

Proof. Differentiating ξ, η and using (5) with the identities $a(\cos 2\varphi \sin\varphi - \sin 2\varphi\cos\varphi) = -\eta$ and $a(\sin 2\varphi\sin\varphi + \cos 2\varphi\cos\varphi) = \xi$ gives the matrix. Its trace is μ and its determinant $\frac{1}{4}\big(\mu^2 - F^2/4 + (\omega-2)^2\big)$, so the eigenvalues are $\mu/2 \pm \frac{1}{2}\sqrt{F^2/4-(\omega-2)^2}$. The statement on the full equation is the averaging theorem for linear periodic systems [16, Ch. 2]. □

3.4 Persistence

Theorem 9 (Persistence for small parameters). *Fix $\mu_0 > 0$, $f > 0$, $\sigma \in \mathbb{R}$ and let $\mu = \varepsilon\mu_0$, $F = \varepsilon f$, $\omega = 2 + \varepsilon\sigma$. There is $\varepsilon_0 > 0$ such that for all $0 < \varepsilon < \varepsilon_0$:*

(a) if $|\sigma| < f/2$, equation (1) has a hyperbolic, asymptotically stable periodic solution $x_+(t)$ of period $4\pi/\omega$ with $x_+(t + 2\pi/\omega) = -x_+(t)$, and

$$x_+(t) = a_+\cos\big(\tfrac{\omega}{2}t + \varphi_s\big) + O(\varepsilon), \qquad \lambda_1 = -(\mu + \mathscr{D}/2) + O(\varepsilon^2),\ \lambda_2 = -\mathscr{D}/2 + O(\varepsilon^2);$$

(b) if moreover $\mathscr{D} < 2\mu$ strictly, there is a hyperbolic saddle periodic solution $x_-(t) = a_-\cos(\frac{\omega}{2}t + \varphi_u) + O(\varepsilon)$ with $\lambda_1 = -(\mu - \mathscr{D}/2) + O(\varepsilon^2)$, $\lambda_2 = +\mathscr{D}/2 + O(\varepsilon^2)$;

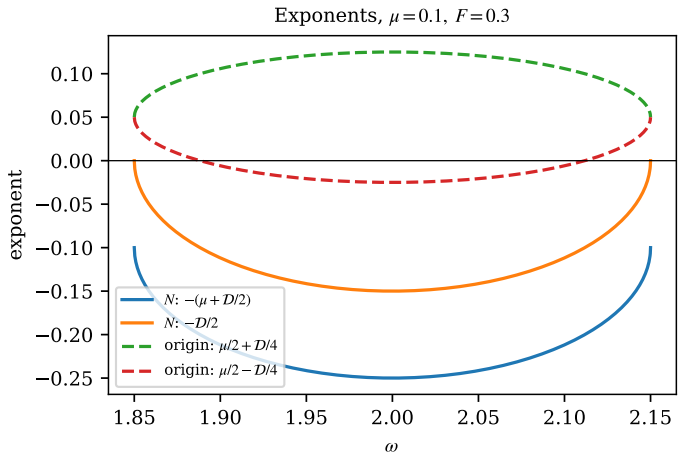

Fig. 3 Exponents of the node N (Theorem 6) and of the origin (Lemma 8) inside the tongue, for $\mu = 0.1$, $F = 0.3$ (closed formulas). The origin exponent $\mu/2 - \mathscr{D}/4$ becomes negative where $\mathscr{D} > 2\mu$.

(c) if $|\sigma| > f/2$, equation (1) has an attracting invariant two-torus, within $O(\varepsilon)$ of the surface $\{x = a_\Gamma(\varphi)\cos(\frac{\omega}{2}t + \varphi)\}$, whose motion has frequencies ω and $\Omega_1 = \frac{\omega}{2} - \operatorname{sgn}(\omega - 2)\,\frac{\kappa}{2} + O(\varepsilon^2)$.

Proof. The change of variables $(x, \dot{x}) \mapsto (a, \varphi)$ is a diffeomorphism on $\{a \geq a_0 > 0\}$ and puts (1) in the form $\dot{z} = \varepsilon h(z,t)$ with h $4\pi/\omega$-periodic in t (after the $O(\varepsilon)$ near-identity transformation). The equilibria N and S and the circle Γ of the averaged system are hyperbolic, with eigenvalues listed in Theorem 6 and with Floquet exponent $-\mu$ transverse to Γ (Theorem 7). The averaging theorem for hyperbolic equilibria [16, Ch. 6] gives (a),(b), while persistence of normally hyperbolic invariant manifolds [18] gives (c). The $O(\varepsilon^2)$ remainders follow from second-order averaging. For the antiperiodicity in (a): the averaged equilibria occur in pairs (a_+, φ_s) and $(a_+, \varphi_s + \pi)$, which correspond to x_+ and $-x_+$ (the circle flow is π-periodic in φ). The time shift $t \mapsto t + T$ increases ψ by π, so it maps the neighbourhood of the first equilibrium to that of the second; by local uniqueness of the hyperbolic periodic orbit, $x_+(t+T) = -x_+(t)$ (Proposition 1(iii)). □

4 Physical relevance and design rules

Where the model appears. Van der Pol–Mathieu dynamics arise whenever a self-excited oscillator has a periodically modulated stiffness. A documented example is the dynamics of dust-acoustic oscillations in a dusty plasma: a multi-fluid model with a source and loss term for the dust grains and a harmonically fluctuating dust charge reduces, for the dust density, to a Van der Pol–Mathieu-type equation [15]. Related self-excited and parametric mechanisms are studied for vertical-axis wind-turbine blades, which can combine cyclic damping, aeroelastic self-excitation and direct excitation [13], and for parametric amplification in Mathieu-type resonators [14]. Equation (1) is the dimensionless normal form of this class; the models in the cited applications contain additional terms, so the results below apply to them at the level of the normal form.

Dimensional form. Consider $z'' - \varepsilon_0(1 - z^2/z_0^2)z' + \omega_0^2\big(1 + h\cos\gamma\tau\big)z = 0$. With $t = \omega_0\tau$, $x = z/z_0$ this is exactly (1) with

$$\mu = \frac{\varepsilon_0}{\omega_0}, \qquad F = h, \qquad \omega = \frac{\gamma}{\omega_0}$$

(the sign of F is irrelevant: $t \mapsto t + \pi/\omega$ changes $F \to -F$). For small μ and F, Theorems 6, 7 and 9 give the following consequences.

(a) *Locking band.* The oscillator is entrained by the parametric modulation (an attracting subharmonic orbit of period $4\pi/\omega$ exists) iff $|\gamma - 2\omega_0| < h\omega_0/2$, i.e. in a band of relative width $h/2$ around $\gamma = 2\omega_0$.

(b) *Amplification.* Inside the band the oscillation amplitude is $z_0 a_+$ with $a_+ = 2\sqrt{1+\mathscr{D}/(2\mu)}$, strictly above the free Van der Pol amplitude $2z_0$ (Remark 1). At the centre the gain over the free cycle is $\sqrt{1+h\omega_0/(2\varepsilon_0)}$; for $\mu = h = 0.1$ it equals $\sqrt{6}/2 \approx 1.22$ (numerical check in Appendix 5, Table 1).

(c) *Avoiding entrainment.* Outside the band the slow flow has the unique attracting orbit of Theorem 7: the amplitude stays on the envelope $a_\Gamma(\varphi)$ around $2z_0$ and the response frequency is $\Omega_1 = \gamma/2 - \operatorname{sgn}(\gamma - 2\omega_0)\,\kappa\omega_0/2$ instead of $\gamma/2$.

(d) *Threshold of the intermediate orbit.* The unstable subharmonic orbit that separates basins exists iff $h < h_c(\gamma) = 2\sqrt{(\gamma/\omega_0 - 2)^2 + (\varepsilon_0/\omega_0)^2}$; at exact resonance $h_c = 2\varepsilon_0/\omega_0$.

5 Conclusions

For the oscillator (1) we have proved that:

1. the trivial solution is always unstable for $\mu > 0$, with exponents $\mu/2 \pm s$ summing exactly to μ (Proposition 2); every periodic orbit satisfies the exact power balance (4) and $\lambda_1 + \lambda_2 = \mu(1 - \langle x^2 \rangle)$;
2. the first-order slow flow is globally solvable: it is triangular, and $u = a^{-2}$ linearises its amplitude equation (Lemma 5);
3. inside the principal tongue $|\omega - 2| < F/2$ the slow flow has a globally attracting node of amplitude $a_+ = 2\sqrt{1+\mathscr{D}/(2\mu)} > 2$, and a saddle of amplitude $a_- = 2\sqrt{1-\mathscr{D}/(2\mu)}$ iff $\mathscr{D} < 2\mu$; both reach the origin on the hyperbola $F^2 = 4(\omega - 2)^2 + 4\mu^2$, where the origin becomes a saddle (Theorem 6, Lemma 8);
4. outside the tongue the slow flow has a unique globally attracting periodic orbit with closed-form amplitude envelope (9), transverse rate μ and phase-rotation frequency $\kappa/2$ (Theorem 7);
5. for small μ and F these objects persist in the full equation as a hyperbolic subharmonic orbit, a saddle orbit and an attracting invariant torus (Theorem 9).

The numerical appendix confirms these first-order predictions and indicates chaos at strong forcing, leading to two open problems (Appendix 5). In summary, multiplying the forcing by the state does not destroy the Van der Pol cycle at weak forcing: it converts it into an amplified, frequency-locked subharmonic orbit inside the 2:1 tongue and into a modulated torus outside it.

APPENDIX

Numerical analysis

Status. Everything in this appendix is numerical evidence obtained with floating-point arithmetic (IEEE double precision, no interval arithmetic). It does not belong to the proofs of Sections 2–3; its role is to test the first-order theory quantitatively, to extend the picture beyond the range of validity of averaging, and to formulate precise open problems (Section 5).

Algorithms

Write (1) as $\dot{z} = f(z,t)$, $z = (x, \dot{x})$, with f T-periodic in t, $T = 2\pi/\omega$, and let Π_T be the stroboscopic (time-T) map, $R(x,v) = (-x,-v)$.

A1 *Integration.* The explicit Runge–Kutta method DOP853 of order 8 with step-size control and dense output [19]; relative tolerance 10^{-11}–10^{-12} and absolute tolerance 10^{-13}–10^{-14} for orbit and Floquet computations. For the parameter scans of A5 a fixed-step classical RK4 scheme with 120–200 steps per forcing period is used.

A2 *Variational equation.* The monodromy matrix is obtained by integrating $\dot{\Phi} = D_z f(z(t),t)\,\Phi$, $\Phi(0) = I$, together with the orbit, where $D_z f = \begin{pmatrix} 0 & 1 \\ -1 + F\cos\omega t - 2\mu x v & \mu(1-x^2) \end{pmatrix}$.

A3 *Subharmonic orbits.* A fixed point $z_* = R\Pi_T(z_*)$ is computed by Newton's method [22] on $\mathscr{G}(z) = R\Pi_T(z) - z$, whose Jacobian is $R\Phi(T) - I$; equivalently $\Pi_{2T}(z_*) = z_*$ with $P = 4\pi/\omega$. The starting point for the stable orbit is the end point of a long transient, and for the saddle orbit the point predicted by Theorem 6, $x = a_- \cos\varphi_u$, $\dot{x} = -a_- \frac{\omega}{2}\sin\varphi_u$. This is the standard shooting approach [23, 24].

A4 *Floquet exponents.* The multipliers $m_{1,2}$ are the eigenvalues of $\Phi(P)$ and $\lambda_j = \ln|m_j|/P$. Exponents of the origin are computed in the same way from the linear equation. The Liouville identity (3) is used as an independent check.

A5 *Largest Lyapunov exponent.* The algorithm of Benettin et al. [20] (see also [21]): a tangent vector is integrated together with the orbit and renormalised once per forcing period; Λ is the average of $\ln\|\cdot\|/T$ after discarding a transient. Locking is tested on the stroboscopic sequence $(-1)^k x(kT)$, which is constant for a locked orbit (Proposition 1).

A6 *Torus quantities.* The frequency Ω_1 is the slope of the unwrapped phase $\arctan 2(-\dot{x}, x)$ over a long window; the amplitude envelope is computed from $\sqrt{x^2 + (\dot{x}/\Omega_1)^2}$ smoothed over one carrier period, and compared with (9), which is evaluated by quadrature (trapezoidal rule on 2×10^4 nodes) and cross-checked against a backward integration of the linear equation for u.

Convergence orders are estimated by least-squares slopes of $\log|\text{error}|$ against $\log\varepsilon$.

The locked orbit

Table 1 compares the amplitude (first Fourier coefficient of x_+ at frequency $\omega/2$) and the two Floquet exponents with Theorem 9(a) at the exact resonance $\omega = 2$.

Table 1 Locked orbit at $\omega = 2$, $\mu = F = \varepsilon$. Predictions: $a_+ = \sqrt{6}$, $\lambda_1 = -\frac{3}{2}\varepsilon$, $\lambda_2 = -\frac{1}{2}\varepsilon$.

ε	a_+ (th.)	a_+ (num.)	$\lvert\Delta a\rvert$	λ_2 (th.)	λ_2 (num.)	λ_1 (th.)	λ_1 (num.)
0.200	2.44949	2.44899	5.0e-04	-0.1000	-0.10303	-0.3000	-0.29709
0.100	2.44949	2.44936	1.3e-04	-0.0500	-0.05037	-0.1500	-0.14964
0.050	2.44949	2.44946	3.2e-05	-0.0250	-0.02505	-0.0750	-0.07496
0.025	2.44949	2.44948	8.0e-06	-0.0125	-0.01251	-0.0375	-0.03749

The amplitude error decays as ε^2 (observed slope 1.99) and the exponent error as ε^3 (slope 3.01) at the resonance centre (Fig. 5). Table 2 repeats the comparison inside the tongue for $\sigma \neq 0$, where the errors are larger: the amplitude error is $O(\varepsilon)$ (at $\sigma = 0.4$ it halves from 0.042 at $\varepsilon = 0.1$ to 0.021 at $\varepsilon = 0.05$), while the exponent error is $O(\varepsilon^2)$ (at $\sigma = 0.4$ it drops from 9.2×10^{-3} to 2.3×10^{-3}), in agreement with Theorem 9(a).

The Liouville identity holds to $\sim 10^{-12}$ in every case, which independently validates the numerics. The leading-order prediction for the sum, $-(\mu + \mathscr{D})$, is reproduced up to $O(\varepsilon^2)$: for $\varepsilon = 0.025$, -0.05000 versus -0.0500002.

Table 2 Locked orbit inside the tongue with detuning $\omega = 2 + \varepsilon\sigma$.

ε	ω	σ	a_+ (th.)	a_+ (num.)	λ_2 (th.)	λ_2 (num.)	λ_1 (th.)	λ_1 (num.)
0.100	2.0250	+0.25	2.3942	2.3706	-0.0433	-0.0445	-0.1433	-0.1366
0.100	1.9750	-0.25	2.3942	2.4178	-0.0433	-0.0427	-0.1433	-0.1497
0.100	2.0400	+0.40	2.2804	2.2380	-0.0300	-0.0297	-0.1300	-0.1208
0.050	2.0200	+0.40	2.2804	2.2592	-0.0150	-0.0149	-0.0650	-0.0627

Table 3 Liouville identity (Prop. 3): sum of the computed Floquet exponents of the locked orbit versus the independently computed orbit average of $\mu(1-x^2)$.

ε	σ	$\lambda_1 + \lambda_2$	$\langle \mu(1-x^2) \rangle$	difference
0.200	+0.00	-0.4001212270	-0.4001212270	1.5e-14
0.100	+0.00	-0.2000155066	-0.2000155066	6.3e-14
0.050	+0.00	-0.1000019494	-0.1000019494	3.6e-14
0.025	+0.00	-0.0500002440	-0.0500002440	1.6e-14
0.100	+0.25	-0.1810425360	-0.1810425360	2.8e-14
0.100	-0.25	-0.1923494582	-0.1923494582	7.7e-14
0.100	+0.40	-0.1504646896	-0.1504646896	1.4e-14
0.050	+0.40	-0.0775999986	-0.0775999986	1.1e-14

The saddle orbit

The saddle orbit cannot be reached by forward integration; it is computed by Newton iteration starting from the predicted initial phase φ_u.

Table 4 Saddle orbit at $\omega = 2$, $\mu = F = \varepsilon$. Predictions: $a_- = \sqrt{2}$, $\lambda = \mp\varepsilon/2$.

ε	a_- (th.)	a_- (num.)	λ_+ (th.)	λ_+ (num.)	λ_- (th.)	λ_- (num.)
0.100	1.41421	1.41399	0.0500	0.04999	-0.0500	-0.04997
0.050	1.41421	1.41416	0.0250	0.02500	-0.0250	-0.02500
0.025	1.41421	1.41420	0.0125	0.01250	-0.0125	-0.01250

The origin, the hyperbola and the tongue boundary

Table 5 Floquet exponents of the origin: leading-order prediction $\mu/2 \pm \mathscr{D}/4$ (inside the tongue) or $\mu/2$ (outside) versus the exact monodromy computation. The last column is $\lambda_+ + \lambda_-$ and equals μ exactly (Prop. 2a).

ε	ω	λ_- (th.)	λ_- (num.)	λ_+ (th.)	λ_+ (num.)	sum
0.100	2.0000	0.02500	0.02502	0.07500	0.07498	0.10000000
0.050	2.0000	0.01250	0.01250	0.03750	0.03750	0.05000000
0.025	2.0000	0.00625	0.00625	0.01875	0.01875	0.02500000
0.100	2.0250	0.02835	0.02920	0.07165	0.07080	0.10000000
0.100	2.0400	0.03500	0.03704	0.06500	0.06296	0.10000000
0.100	2.0600	0.05000	0.05000	0.05000	0.05000	0.10000000
0.100	2.1000	0.05000	0.05000	0.05000	0.05000	0.10000000

The hyperbola prediction is exact at the centre to 0.05% and degrades to $\approx 4\%$ at $|\omega - 2| = 0.2$, where $F \approx 0.45$ is no longer small: the error is a second-order effect, consistent with the use of a first-order averaged

Table 6 Hyperbola $F = 2\sqrt{(\omega-2)^2+\mu^2}$ ($\mu = 0.1$): theory versus the root of $\lambda_-(F) = 0$ obtained from the exact monodromy.

ω	F (theory)	F (numerical root)	rel. error (%)
1.80	0.44721	0.43432	2.88
1.84	0.37736	0.36706	2.73
1.88	0.31241	0.30461	2.50
1.92	0.25612	0.25077	2.09
1.96	0.21541	0.21263	1.29
2.00	0.20000	0.20011	0.05
2.04	0.21541	0.21848	1.43
2.08	0.25612	0.26209	2.33
2.12	0.31241	0.32151	2.91
2.16	0.37736	0.39021	3.41
2.20	0.44721	0.46467	3.90

system.

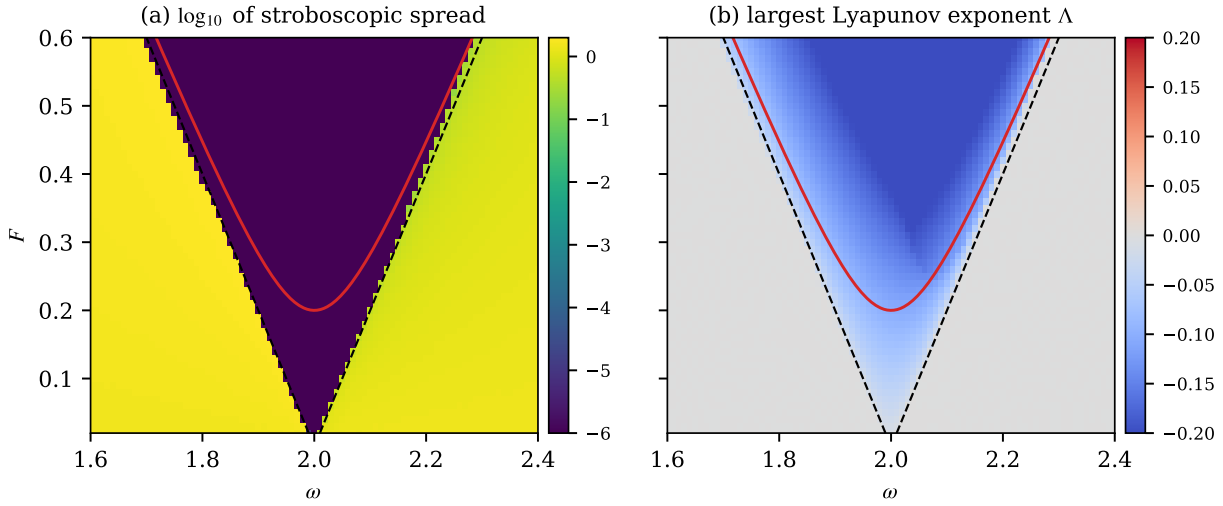

Fig. 4 Locking map for $\mu = 0.1$ (81×59 grid in (ω, F)). (a) Spread of the stroboscopic sequence $(-1)^k x(kT)$; dark = locked ($< 10^{-3}$). (b) Largest Lyapunov exponent Λ. Dashed lines: $|\omega - 2| = F/2$; red: hyperbola $F = 2\sqrt{(\omega-2)^2+\mu^2}$.

Table 7 summarises the classification of $N = 4779$ grid points by direct simulation against the prediction "locked iff $|\omega - 2| < F/2$".

For $F \le 0.3$ the disagreements are confined to grid points lying exactly on the edge.

Quasi-periodic regime

As a self-consistency check, the closed form (9) was compared with a direct high-precision integration of the linear equation $\mathrm{d}u/\mathrm{d}\varphi = (2/q)(gu - \mu/4)$ (integrated backwards, where it is stable): the amplitude extrema agree to 2×10^{-7} (1.8350871 and 2.1523140 against 1.8350872 and 2.1523138). The frequency error decays as ε^2 (slope 1.97), in agreement with Theorem 9(c).

Table 7 Locking classification, $\mu = 0.1$, $\omega \in [1.6, 2.4]$, $F \in [0.02, 0.6]$.

Quantity	Value
Grid points	4779
Locked (simulation)	1822
Inside the predicted tongue	1824
Agreement (both locked and inside, or neither)	98.8 %
Disagreements	58 (all within one grid cell, $\Delta\omega = 0.01$, of the edge)
Max. disagreement distance $\big\lvert\lvert\omega - 2\rvert - F/2\big\rvert$	0.010
Locked: largest Lyapunov exponent range	$[-0.354, -0.005]$
Unlocked: $\max\Lambda$ (numerical zero)	0.0024
Chaotic points ($\Lambda > 0.005$)	0

Table 8 Quasi-periodic regime, $\sigma = 3$, $\mu = F = \varepsilon$. Torus frequency Ω_1 and amplitude extrema of the envelope; the theoretical extrema $a_{\min} = 1.8351$, $a_{\max} = 2.1523$ come from (9) (they do not depend on ε in the slow scaling).

ε	ω	Ω_1 (th.)	Ω_1 (num.)	$\lvert\Delta\Omega_1\rvert$	$a_{\min}$ (th.)	$a_{\min}$ (num.)	$a_{\max}$ (th.)	$a_{\max}$ (num.)
0.1000	2.3000	1.00210	1.00126	8.4e-04	1.8351	1.8600	2.1523	2.1348
0.0500	2.1500	1.00105	1.00083	2.1e-04	1.8351	1.8420	2.1523	2.1481
0.0250	2.0750	1.00052	1.00047	5.5e-05	1.8351	1.8371	2.1523	2.1514
0.0125	2.0375	1.00026	1.00025	1.4e-05	1.8351	1.8357	2.1523	2.1521

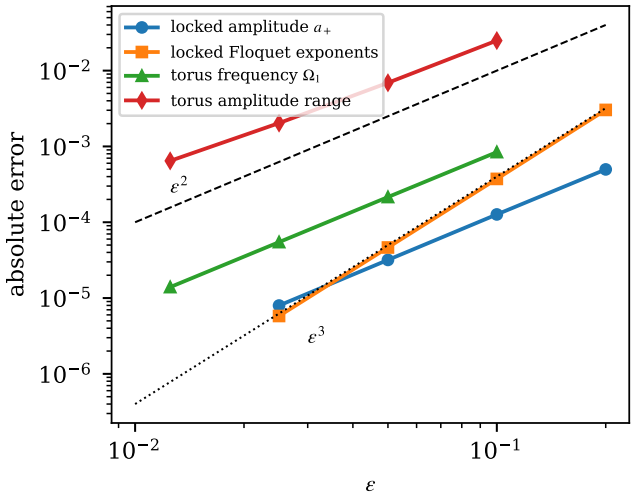

Fig. 5 Absolute errors of the first-order predictions versus ε (log–log). Dashed: ε^2; dotted: ε^3. Observed slopes: amplitude 1.99, locked Floquet exponents 3.01, torus frequency 1.97, torus amplitude range 1.76.

Strong forcing: Lyapunov maps and periodic windows

The results of Sections 2–3 are asymptotic in ε. For larger μ and F the averaged picture is no longer predictive, and the evidence below indicates chaotic dynamics. These statements are numerical evidence, not theorems.

Lyapunov maps. Figure 7 shows the largest Lyapunov exponent Λ (per unit time, Benettin algorithm [20], 300–500 forcing periods after transients) over $\omega \in [0.6, 3]$, $F \in [0.1, 3]$. For $\mu = 0.5$ the fraction of grid points with $\Lambda > 0.01$ is 4.8% (173/3599, $\max\Lambda = 0.135$); for $\mu = 1$ it is 7.6% (275/3599, $\max\Lambda = 0.200$). No unbounded orbit was detected: for the initial condition used, the maximum stroboscopic value of $|x|$ over all

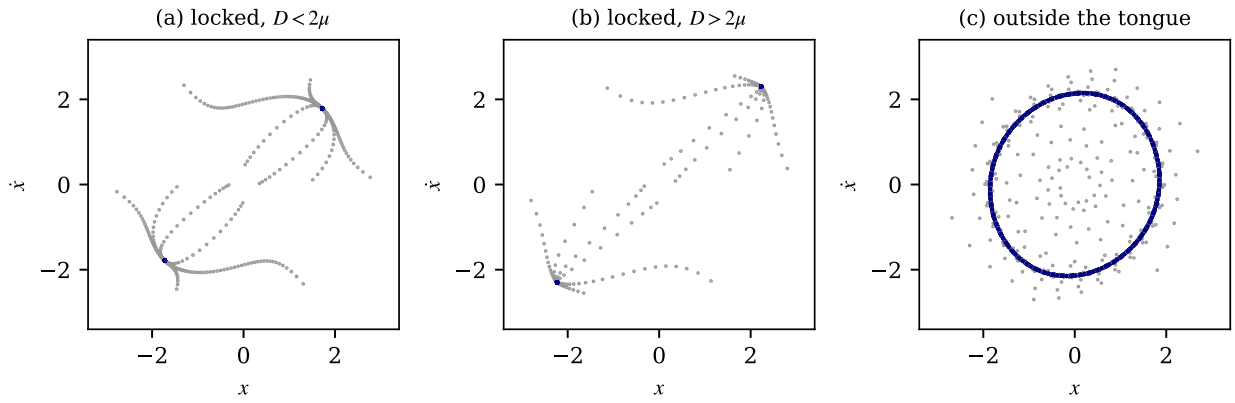

Fig. 6 Stroboscopic sections $(x(kT),\dot{x}(kT))$ for $\varepsilon = 0.05$: (a) $\mu = F = \varepsilon$, $\omega = 2$ ($\mathscr{D} < 2\mu$): all orbits converge to the two points of the locked orbit ($\pm$ symmetry, Prop. 1); (b) $\mu = \varepsilon$, $F = 3\varepsilon$ ($\mathscr{D} > 2\mu$): same picture, no saddle; (c) $\omega = 2+3\varepsilon$: invariant closed curve (torus section). Grey: transient, blue: final 120 iterates.

scans was 3.52 ($\mu = 0.1$), 4.25 ($\mu = 0.5$) and 3.38 ($\mu = 1$).

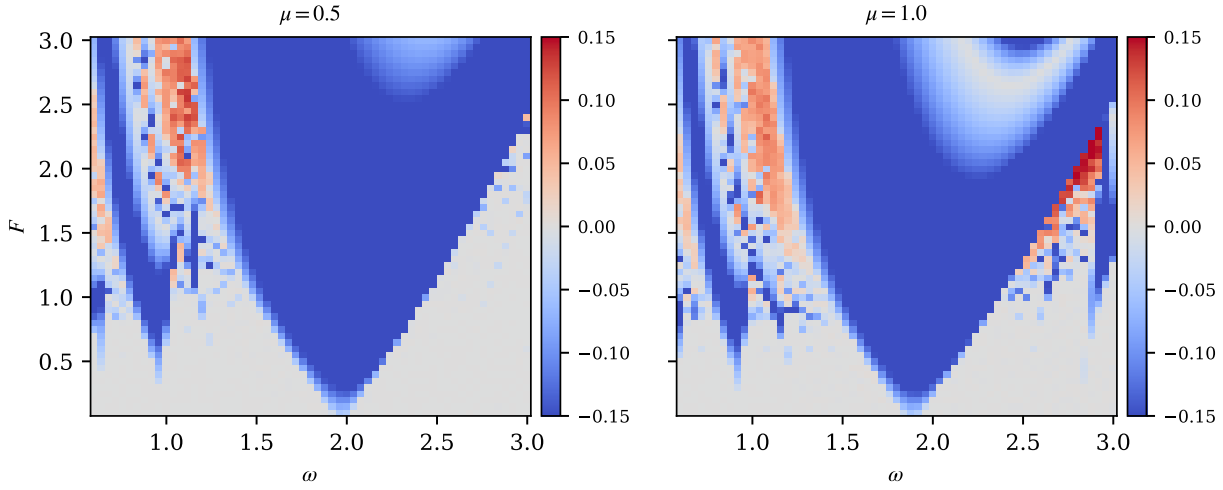

Fig. 7 Largest Lyapunov exponent in the (ω, F)-plane. Red: $\Lambda > 0$ (chaos); blue: $\Lambda < 0$ (periodic); white: $\Lambda \approx 0$ (quasi-periodic). Left: $\mu = 0.5$; right: $\mu = 1$ (49×40 grid).

Route along F. Figure 8 follows $F \in [0.3, 1.6]$ at $\mu = 1$, $\omega = 1$ (521 values). For $F \lesssim 0.78$ the attractor is a torus ($|\Lambda| < 1.3 \times 10^{-3}$); at $F \approx 0.80$ the dynamics locks ($\Lambda < -0.02$ from $F = 0.8025$), and for larger F periodic windows alternate with chaotic bands: 60 of the 521 values have $\Lambda > 0.01$, with $\max \Lambda = 0.081$ at $F = 1.555$.

Independent verification. Table 9 compares the fixed-step RK4 results used for the maps with a second integration based on the adaptive 8th-order method with 1500 forcing periods. The sign is the same in all four tested cases, and the values agree within the finite-time variability of Λ.

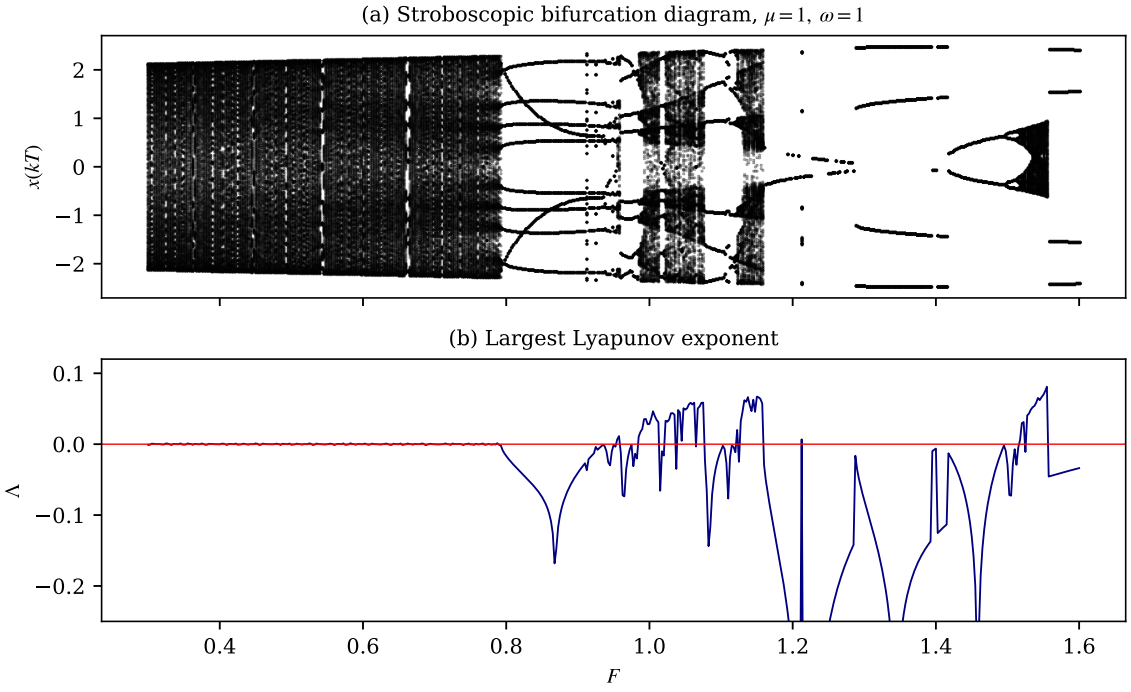

Fig. 8 (a) Stroboscopic bifurcation diagram, $\mu = 1$, $\omega = 1$. (b) Largest Lyapunov exponent.

Table 9 Independent confirmation of positive Lyapunov exponents.

μ	ω	F	Λ (RK4, 200 periods)	Λ (DOP853, 1500 periods)
1.0	1.00	1.05	0.0558	0.0532
1.0	1.00	1.00	0.0242	0.0293
0.5	1.04	1.20	0.0484	0.0476
0.5	0.72	1.25	0.0170	0.0172

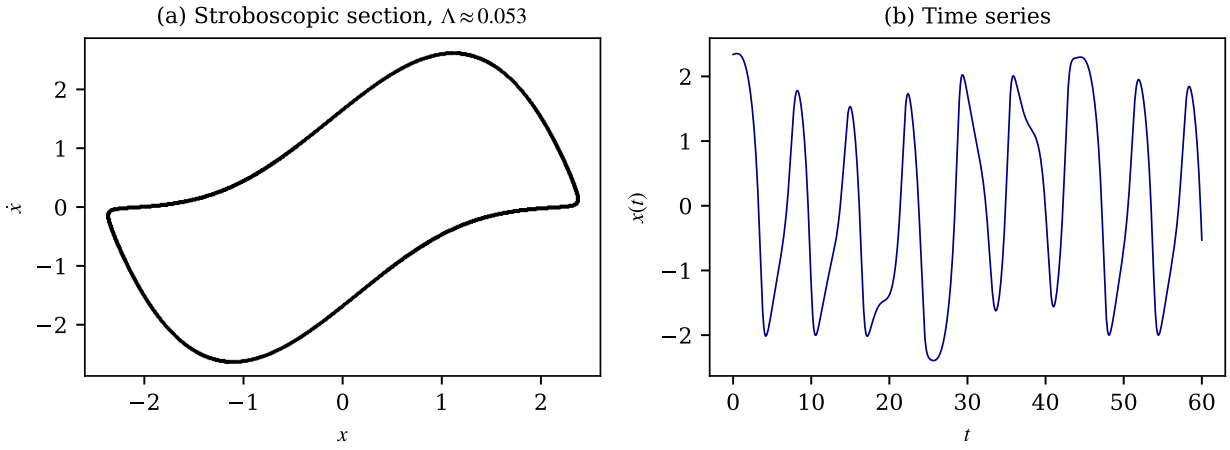

Fig. 9 Chaotic regime, $\mu = 1$, $\omega = 1$, $F = 1.05$ ($\Lambda \approx 0.053$). (a) Stroboscopic section (1.5×10^5 points from 300 initial conditions: all lie on the same folded, nearly one-dimensional set). (b) Time series.

Open Problems

Two precise questions are raised by the numerical evidence above; neither is addressed by the theorems of this paper.

Definition 1 (Setting)**.** Let $\mu = 1$, $\omega = 1$ and consider (1) as a family in F.

Open Problem 1 (Chaos)**.** *Fig. 8 and Table 9 indicate a positive Lyapunov exponent on a set of F-values in* $[0.95, 1.56]$*, interleaved with periodic windows. Prove that for some (and describe the set of) parameter values* (μ, ω, F) *the stroboscopic map* Π_T *has a transversal homoclinic point to a hyperbolic periodic orbit, hence a Smale horseshoe.*

Open Problem 2 (Dissipativity)**.** *In all* $\sim 10^4$ *integrations performed, the trajectories remained bounded (maximum stroboscopic* $|x|$ *below* 4.3*). Prove or disprove that for every* $\mu > 0$*,* $F \geq 0$*,* $\omega > 0$ *the stroboscopic map* Π_T *possesses a bounded absorbing set, i.e. system* (1) *is dissipative in the sense of Levinson.*

References

[1] B. van der Pol, On relaxation-oscillations, *Philosophical Magazine* **2** (1926), 978–992.
[2] É. Mathieu, Mémoire sur le mouvement vibratoire d'une membrane de forme elliptique, *J. Math. Pures Appl.* **13** (1868), 137–203.
[3] W. Magnus, S. Winkler, *Hill's Equation*, Interscience, New York, 1966.
[4] I. Kovačić, R. Rand, S. Mohamed Sah, Mathieu's equation and its generalizations: overview of stability charts and their features, *Appl. Mech. Rev.* **70** (2018), 020802.
[5] A. H. Nayfeh, D. T. Mook, *Nonlinear Oscillations*, Wiley, New York, 1979.
[6] J. Guckenheimer, P. Holmes, *Nonlinear Oscillations, Dynamical Systems, and Bifurcations of Vector Fields*, Springer, New York, 1983.
[7] F. Veerman, F. Verhulst, Quasiperiodic phenomena in the Van der Pol–Mathieu equation, *J. Sound Vib.* **326** (2009), 314–320.
[8] M. Belhaq, A. Fahsi, 2:1 and 1:1 frequency-locking in fast excited van der Pol–Mathieu equation, *Nonlinear Dyn.* **53** (2008), 139–152.
[9] R. H. Rand, K. Guennoun, M. Belhaq, 2:2:1 resonance in the quasi-periodic Mathieu equation, *Nonlinear Dyn.* **31** (2003).
[10] M. Pandey, R. H. Rand, A. T. Zehnder, Frequency locking in a forced Mathieu–van der Pol–Duffing system, *Nonlinear Dyn.* **54** (2008), 3–12.
[11] J. Warmiński, Nonlinear dynamics of self-, parametric, and externally excited oscillator with time delay: van der Pol versus Rayleigh models, *Nonlinear Dyn.* **99** (2020), 35–56.
[12] J. Huang, T. Wang, S. Chen, Nonlinear dynamic analysis of a van der Pol–Mathieu equation with external excitation, *Chinese J. Theor. Appl. Mech.* **53** (2021), 496–510, doi:10.6052/0459-1879-20-310.
[13] F. Afzali, E. Kharazmi, B. F. Feeny, Resonances of a forced van der Pol equation with parametric damping, *Nonlinear Dyn.* **111** (2023), 5269–5285.
[14] V. Ramakrishnan, B. F. Feeny, Primary parametric amplification in a weakly forced Mathieu equation, *J. Vib. Acoust.* **144** (2022), 051006.
[15] M. Momeni, I. Kourakis, M. Moslehi-Fard, P. K. Shukla, A Van der Pol–Mathieu equation for the dynamics of dust grain charge in dusty plasmas, *J. Phys. A: Math. Theor.* **40** (2007), F473–F481.
[16] J. A. Sanders, F. Verhulst, J. Murdock, *Averaging Methods in Nonlinear Dynamical Systems*, 2nd ed., Springer, New York, 2007.
[17] F. Verhulst, *Nonlinear Differential Equations and Dynamical Systems*, 2nd ed., Springer, Berlin, 1996.
[18] N. Fenichel, Persistence and smoothness of invariant manifolds for flows, *Indiana Univ. Math. J.* **21** (1971), 193–226.
[19] E. Hairer, S. P. Nørsett, G. Wanner, *Solving Ordinary Differential Equations I: Nonstiff Problems*, 2nd ed., Springer, Berlin, 1993.
[20] G. Benettin, L. Galgani, A. Giorgilli, J.-M. Strelcyn, Lyapunov characteristic exponents for smooth dynamical systems and for Hamiltonian systems; a method for computing all of them, *Meccanica* **15** (1980), 9–20.
[21] J.-P. Eckmann, D. Ruelle, Ergodic theory of chaos and strange attractors, *Rev. Mod. Phys.* **57** (1985), 617–656.
[22] P. Deuflhard, *Newton Methods for Nonlinear Problems*, Springer, Berlin, 2004.
[23] T. S. Parker, L. O. Chua, *Practical Numerical Algorithms for Chaotic Systems*, Springer, New York, 1989.
[24] R. Seydel, *Practical Bifurcation and Stability Analysis*, 3rd ed., Springer, New York, 2010.